

Adversarial Distributional Training for Robust Deep Learning

Zhijie Deng^{*1} Yinpeng Dong^{*1} Tianyu Pang¹ Hang Su¹ Jun Zhu¹

Abstract

Adversarial training (AT) is among the most effective techniques to improve model robustness by augmenting training data with adversarial examples. However, the adversarially trained models do not perform well enough on test data or under other attack algorithms unseen during training, which remains to be improved. In this paper, we introduce a novel *adversarial distributional training* (ADT) framework for learning robust models. Specifically, we formulate ADT as a minimax optimization problem, where the inner maximization aims to learn an adversarial distribution to characterize the potential adversarial examples around a natural one, and the outer minimization aims to train robust classifiers by minimizing the expected loss over the worst-case adversarial distributions. We conduct a theoretical analysis on how to solve the minimax problem, leading to a general algorithm for ADT. We further propose three different approaches to parameterize the adversarial distributions. Empirical results on various benchmarks validate the effectiveness of ADT compared with the state-of-the-art AT methods.

1. Introduction

Recent breakthroughs in deep neural networks (DNNs) have led to substantial success in a wide range of fields, including computer vision (Krizhevsky et al., 2012; He et al., 2016), speech recognition (Graves et al., 2013), natural language processing (Devlin et al., 2019), etc. However, DNN models are vulnerable to adversarial examples (Szegedy et al., 2014; Goodfellow et al., 2015), which are indistinguishable from natural examples but make a model produce erroneous predictions. The adversarial vulnerability of DNNs limits their practical applicability for various security-sensitive applications, such as autonomous driving, healthcare, and

finance. Therefore, it is essential to develop robust DNN models that are resistant to adversarial examples.

Considerable efforts have been devoted to improving the adversarial robustness of DNNs (Goodfellow et al., 2015; Papernot et al., 2016; Kurakin et al., 2017; Liao et al., 2018; Madry et al., 2018; Wong & Kolter, 2018; Pang et al., 2019; Zhang et al., 2019). Among them, adversarial training (AT) is one of the most effective techniques (Athalye et al., 2018). Specifically, AT can be formulated as a minimax optimization problem (Madry et al., 2018), where the inner maximization aims to find an adversarial example that maximizes the classification loss for a natural one, while the outer minimization aims to optimize the model parameters using the adversarial examples to train a robust classifier. To solve the non-concave and typically intractable inner maximization problem approximately, several adversarial attack methods can be adopted, such as fast gradient sign method (FGSM) (Goodfellow et al., 2015), projected gradient descent method (PGD) (Madry et al., 2018).

However, the performance of the state-of-the-art AT methods is still unsatisfactory by showing only a modest level of adversarial robustness. Recent work improves AT by exploiting more labeled and unlabeled data (Hendrycks et al., 2019; Alayrac et al., 2019; Carmon et al., 2019). Nevertheless, in this work we focus on designing a more effective training mechanism to tackle this problem, which is orthogonal to previous work on using more data. Moreover, most AT methods solve the inner maximization using a specific attack, which can result in poor generalization for other attacks under the same threat model (Song et al., 2019). For example, defenses trained on the naive FGSM adversarial examples, without random initialization or early stopping (Wong et al., 2020), are vulnerable to multi-step attacks (Kurakin et al., 2017; Tramèr et al., 2018). Although PGD is commonly adopted to evaluate the robustness of AT-based defenses, some methods (e.g., Zhang & Wang (2019)) that achieve the state-of-the-art robustness against PGD can still be defeated by other attacks¹. It indicates that these defenses probably cause gradient masking (Tramèr et al., 2018; Athalye et al., 2018; Uesato et al., 2018), and may be fooled by stronger or adaptive attacks. In summary, there is still

^{*}Equal contribution ¹Dept. of Comp. Sci. & Tech., BNRist Center, Institute for AI, THBI Lab, Tsinghua University, Beijing, 100084, China. Correspondence to: Yinpeng Dong <dyp17@mails.tsinghua.edu.cn>, Jun Zhu <dc-szj@mail.tsinghua.edu.cn>.

¹A discussion on it can be found at <https://openreview.net/forum?id=Syzej0NYvr¬eId=rkeBhuBMjS>.

a generalization problem across attacks in the existing AT methods. It should be noted that we consider the generalization problem across attacks *under the same threat model*, rather than studying the generalization ability *across different threat models* (Hendrycks & Dietterich, 2019; Engstrom et al., 2019; Tramèr & Boneh, 2019).

To mitigate the aforementioned problems of AT and improve the model robustness against all possible adversarial attacks, in this paper we introduce a novel *adversarial distributional training* (ADT) framework. Unlike AT, we formulate ADT as a different minimax optimization problem, where we model the adversarial examples in the vicinity of a natural input using a distribution. This distribution is capable of characterizing heterogeneous adversarial examples around the natural one. Then, the inner maximization problem of ADT corresponds to finding an adversarial distribution for each natural example by maximizing the expected loss over this distribution, and the outer minimization problem aims to learn a robust classifier by minimizing the expected loss over the worst-case adversarial distributions.

Compared with the vanilla AT that generates an adversarial example for each input using a single attack, ADT learns an adversarial distribution that assigns probabilities for a large adversarial region. This region potentially contains adversarial examples given by various attack methods, such that minimizing the expected loss over this region would lead to a better generalization ability across attacks. Moreover, the region covered by the adversarial distribution can help to learn a smooth and flattened loss surface in the input space, as shown in Figure 4. Consequently, ADT can improve the overall robustness of the trained models over AT, without sacrificing natural accuracy.

We perform a theoretical analysis on how to solve the minimax optimization problem in ADT, which indicates that the minimax problem can be solved in a sequential manner similar to AT (Madry et al., 2018), leading to a general algorithm for ADT. In particular, we can first find a maximizer (i.e., an adversarial distribution) of the inner problem and then update the model parameters along the gradient direction of the loss function at the maximizer of the inner problem. In this paper, we implement ADT by parameterizing the adversarial distributions with trainable parameters and propose three different approaches to specify the parameterization techniques and learning strategies, respectively.

We conduct extensive experiments and robustness evaluations on the CIFAR-10, CIFAR-100 (Krizhevsky & Hinton, 2009), and SVHN (Netzer et al., 2011) datasets to empirically compare the adversarial robustness of the defense models trained by ADT with the alternative state-of-the-art AT models under both white-box attacks and black-box attacks. The results validate the effectiveness of our proposed methods on building robust deep learning models.

2. Proposed Method

In this section, we first introduce the background knowledge of adversarial training (AT), then detail the proposed adversarial distributional training (ADT) framework, and finally provide a general algorithm for solving ADT.

2.1. Adversarial Training

Adversarial training has been widely studied to improve the adversarial robustness of DNNs. Given a dataset $\mathcal{D} = \{(\mathbf{x}_i, y_i)\}_{i=1}^n$ of n training samples with $\mathbf{x}_i \in \mathbb{R}^d$ and $y_i \in \{1, \dots, C\}$ respectively being the natural example and the corresponding label, AT can be formulated as a minimax optimization problem (Madry et al., 2018) as

$$\min_{\theta} \frac{1}{n} \sum_{i=1}^n \max_{\delta_i \in \mathcal{S}} \mathcal{L}(f_{\theta}(\mathbf{x}_i + \delta_i), y_i), \quad (1)$$

where f_{θ} is the DNN model with parameters θ that outputs predicted probabilities over all classes, \mathcal{L} is a loss function (e.g., cross-entropy loss), and $\mathcal{S} = \{\delta : \|\delta\|_{\infty} \leq \epsilon\}$ is a set of allowed perturbations with ϵ being the perturbation budget. While we only focus on the ℓ_{∞} norm constraint in this paper, the extension to other norms is straightforward.

This minimax problem is usually solved sequentially, i.e., adversarial examples are crafted by solving the inner maximization first, and then the model parameters are optimized based on the generated adversarial examples. Several attack methods can be used to solve the inner maximization problem approximately. The fast gradient sign method (FGSM) (Goodfellow et al., 2015) generates the adversarial perturbation δ_i^* using the loss gradient with respect to the input as

$$\delta_i^* = \epsilon \cdot \text{sign}(\nabla_{\mathbf{x}} \mathcal{L}(f_{\theta}(\mathbf{x}_i), y_i)). \quad (2)$$

The projected gradient descent method (PGD) (Madry et al., 2018) takes multiple gradient steps as

$$\delta_i^{t+1} = \Pi_{\mathcal{S}}(\delta_i^t + \alpha \cdot \text{sign}(\nabla_{\mathbf{x}} \mathcal{L}(f_{\theta}(\mathbf{x}_i + \delta_i^t), y_i))), \quad (3)$$

where δ_i^t is the adversarial perturbation at the t -th step, $\Pi(\cdot)$ is the projection function, and α is a small step size. δ_i^0 is initialized uniformly in \mathcal{S} . For the T -step PGD, the final adversarial perturbation is given by $\delta_i^* = \delta_i^T$.

2.2. Adversarial Distributional Training

As we discussed, though effective, AT is not problemless. On one hand, the performance of the state-of-the-art AT methods is far from satisfactory. On the other hand, the generalization ability across attacks is poor. To alleviate these problems, we propose to capture the distribution of adversarial perturbations around each input instead of only finding a locally most adversarial point for more generalizable adversarial training, which is named as *adversarial distributional*

training (ADT). In particular, we model the adversarial perturbations around each natural example \mathbf{x}_i by a distribution $p(\delta_i)$, whose support is contained in \mathcal{S} . Based on this, ADT is formulated as the following distribution-based minimax optimization problem as

$$\min_{\theta} \frac{1}{n} \sum_{i=1}^n \max_{p(\delta_i) \in \mathcal{P}} \mathbb{E}_{p(\delta_i)} [\mathcal{L}(f_{\theta}(\mathbf{x}_i + \delta_i), y_i)], \quad (4)$$

where $\mathcal{P} = \{p : \text{supp}(p) \subseteq \mathcal{S}\}$ is the set of all possible distributions with support contained in \mathcal{S} . As can be seen in Eqn. (4), the inner maximization aims to learn an adversarial distribution, such that a point drawn from it is likely an adversarial example. And the objective of the outer minimization is to adversarially train the model parameters by minimizing the expected loss over the worst-case adversarial distributions induced by the inner problem.

The major difference between AT and ADT is that for each natural input \mathbf{x}_i , AT finds a worst-case adversarial example, while ADT learns a worst-case adversarial distribution that assigns probabilities for a relatively large adversarial region contained in \mathcal{S} . Because adversarial examples can be generated by various methods, we would expect that those adversarial examples probably lie in the region covered by the distribution. Training on the expected loss over this distribution can naturally lead to a better generalization ability across attacks under the same threat model.

Furthermore, ADT is likely to be more effective than the vanilla AT. The main reasons are as follows. AT in Eqn. (1) only concerns the robustness at a locally most adversarial point, but new adversarial examples may also emerge in other regions due to the high non-linearity of DNNs. Although PGD is shown to be a universal first-order adversary (Madry et al., 2018), robustness against PGD cannot confer robustness to attacks beyond the first-order adversaries. But the adversarial distribution learned in ADT can characterize adversarial examples in a large region, some of which are not reachable by the first-order adversaries since they are not local maximizers of the inner problem of AT. Training on the expected loss over the adversarial distribution can consequently help to learn a smoother and more flattened loss surface around the natural examples in the input space, as shown in Figure 4. Therefore, ADT can improve the overall robustness compared with AT.

2.3. Regularizing Adversarial Distributions

For the inner maximization of ADT, we can easily see that

$$\begin{aligned} & \max_{p(\delta_i) \in \mathcal{P}} \mathbb{E}_{p(\delta_i)} [\mathcal{L}(f_{\theta}(\mathbf{x}_i + \delta_i), y_i)] \\ & \leq \max_{\delta_i \in \mathcal{S}} \mathcal{L}(f_{\theta}(\mathbf{x}_i + \delta_i), y_i). \end{aligned} \quad (5)$$

It indicates that the optimal distribution by solving the inner problem of ADT will degenerate into a Dirac distribution.

Hence the adversarial distribution cannot cover a diverse set of adversarial examples, and ADT becomes AT.

To solve the degeneration issue, we add an entropic regularization term into the training objective (4) of ADT as

$$\min_{\theta} \frac{1}{n} \sum_{i=1}^n \max_{p(\delta_i) \in \mathcal{P}} \mathcal{J}(p(\delta_i), \theta), \quad \text{with} \quad (6)$$

$\mathcal{J}(p(\delta_i), \theta) = \mathbb{E}_{p(\delta_i)} [\mathcal{L}(f_{\theta}(\mathbf{x}_i + \delta_i), y_i)] + \lambda \mathcal{H}(p(\delta_i))$, where $\mathcal{H}(p(\delta_i)) = -\mathbb{E}_{p(\delta_i)} [\log p(\delta_i)]$ is the entropy of $p(\delta_i)$ to increase its support and avoid the degeneration problem. λ is a balancing hyperparameter. In Eqn. (6), we let $\mathcal{J}(p(\delta_i), \theta)$ denote the overall loss function for notation simplicity. We next provide a theoretical analysis on how to solve problem (6), which leads to a general algorithm.

2.4. A General Algorithm for ADT

To solve minimax optimization problems, Danskin’s theorem (Danskin, 2012) states how the maximizers of the inner problem can be used to define the gradient directions for the outer problem, which is also the theoretical foundation of AT (Madry et al., 2018). But it is problematic to directly apply Danskin’s theorem for solving ADT since the searching space \mathcal{P} of the inner problem does not meet the exact assumptions of this theorem. As it is non-trivial to perform a theoretical analysis on how to solve ADT, we first lay out the following assumptions.

Assumption 1. *The loss function $\mathcal{J}(p(\delta_i), \theta)$ is continuously differentiable with respect to θ .*

Assumption 1 is also made in Madry et al. (2018) for AT. Although the loss function is not completely continuously differentiable due to the ReLU layers, the set of discontinuities has measure zero, such that it is assumed not to be an issue in practice (Madry et al., 2018).

Assumption 2. *The probability density functions of distributions in \mathcal{P} are bounded and equicontinuous.*

Assumption 2 puts a restriction on the set of distributions \mathcal{P} . We show that the explicit adversarial distributions proposed in Section 3.1 satisfy this assumption (in Appendix A.1).

Given these assumptions, we have the following theorem.

Theorem 1. *Suppose Assumptions 1 and 2 hold. We define $\rho(\theta) = \max_{p(\delta_i) \in \mathcal{P}} \mathcal{J}(p(\delta_i), \theta)$, and $\mathcal{P}^*(\theta) = \{p(\delta_i) \in \mathcal{P} : \mathcal{J}(p(\delta_i), \theta) = \rho(\theta)\}$. Then $\rho(\theta)$ is directionally differentiable, and its directional derivative along the direction \mathbf{v} satisfies*

$$\rho'(\theta; \mathbf{v}) = \sup_{p(\delta_i) \in \mathcal{P}^*(\theta)} \mathbf{v}^{\top} \nabla_{\theta} \mathcal{J}(p(\delta_i), \theta). \quad (7)$$

In particular, when the set $\mathcal{P}^(\theta) = \{p^*(\delta_i)\}$ only contains one maximizer, $\rho(\theta)$ is differentiable at θ and*

$$\nabla_{\theta} \rho(\theta) = \nabla_{\theta} \mathcal{J}(p^*(\delta_i), \theta). \quad (8)$$

Algorithm 1 The general algorithm for ADT

Input: Training data \mathcal{D} , objective function $\mathcal{J}(p(\delta_i), \theta)$, the set of perturbation distributions \mathcal{P} , training epochs N , and learning rate η .

Initialize θ ;

for epoch = 1 **to** N **do**

for each minibatch $\mathcal{B} \subset \mathcal{D}$ **do**

 Obtain $p^*(\delta_i)$ for each input $(\mathbf{x}_i, y_i) \in \mathcal{B}$ by solving

$$p^*(\delta_i) = \arg \max_{p(\delta_i) \in \mathcal{P}} \mathcal{J}(p(\delta_i), \theta).$$

 Update θ with stochastic gradient descent

$$\theta \leftarrow \theta - \eta \cdot \mathbb{E}_{(\mathbf{x}_i, y_i) \in \mathcal{B}} [\nabla_{\theta} \mathcal{J}(p^*(\delta_i), \theta)].$$

end for

end for

The complete proof of Theorem 1 is deferred to Appendix A.1. Theorem 1 provides us a general principle for training ADT, by first solving the inner problem and then updating the model parameters along the gradient direction of the loss function at the global maximizer of the inner problem, in a sequential manner similar to AT (Madry et al., 2018). We provide the general algorithm for ADT in Alg. 1. Similar to AT, the global maximizer of the inner problem cannot be solved analytically. Therefore, we propose three different approaches to obtain approximate solutions, as introduced in Section 3. Although we cannot reach the global maximizer of the inner problem, our experiments suggest that we can reliably solve the minimax problem (6) by our algorithm.

3. Parameterizing Adversarial Distributions

At the core of ADT lie the solutions of the inner maximization problem of Eqn. (6). The basic idea is to parameterize the adversarial distributions with trainable parameters ϕ_i . With the parameterized $p_{\phi_i}(\delta_i)$, the inner problem is converted into maximizing the expected loss with respect to ϕ_i . In the following subsections, we elaborate three different approaches to specify the detailed parametrizations and corresponding learning strategies, respectively. We provide an overview of these approaches in Figure 1.

3.1. Explicit Modeling of Adversarial Perturbations

A natural way to model adversarial perturbations around an input is using a distribution with an explicit density function. We name ADT with EXPLICIT adversarial distributions as ADT_{EXP}. To define a proper distribution $p_{\phi_i}(\delta_i)$ on \mathcal{S} , we take the transformation of random variable approach as

$$\delta_i = \epsilon \cdot \tanh(\mathbf{u}_i), \quad \mathbf{u}_i \sim \mathcal{N}(\mu_i, \text{diag}(\sigma_i^2)), \quad (9)$$

where \mathbf{u}_i is sampled from a diagonal Gaussian distribution with $\mu_i, \sigma_i \in \mathbb{R}^d$ as the mean and standard deviation. \mathbf{u}_i is transformed by a tanh function and then multiplied by

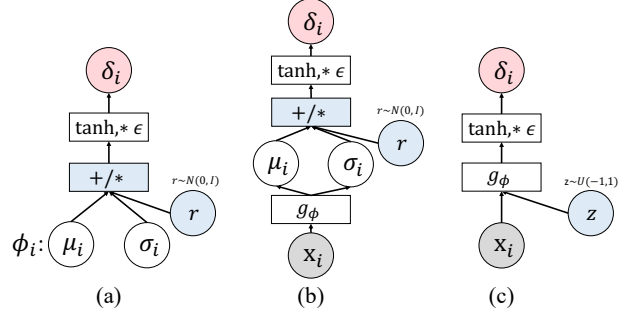


Figure 1. An illustration of the three different approaches to parameterize the distributions of adversarial perturbations. (a) ADT_{EXP}: the explicit adversarial distribution $p_{\phi_i}(\delta_i)$ is defined by transforming $\mathcal{N}(\mu_i, \text{diag}(\sigma_i^2))$ via tanh followed by a multiplication with ϵ . (b) ADT_{EXP-AM}: we amortize the explicit adversarial distributions by a neural network g_ϕ taking \mathbf{x}_i as input. (c) ADT_{IMP-AM}: we define the implicit adversarial distributions by inputting an additional random variable $\mathbf{z} \sim \mathcal{U}(-1, 1)$ to the network g_ϕ .

ϵ to get δ_i . We let $\phi_i = (\mu_i, \sigma_i)$ denote the parameters to be learned. We sample \mathbf{u}_i from a diagonal Gaussian mainly for the sake of computational simplicity. But our method is fully compatible with more expressive distributions, such as matrix-variate Gaussians (Louizos & Welling, 2016) or multiplicative normalizing flows (Louizos & Welling, 2017), and we leave using them for future work.

Given Eqn. (9), the inner problem of Eqn. (6) becomes

$$\max_{\phi_i} \left\{ \mathbb{E}_{p_{\phi_i}(\delta_i)} [\mathcal{L}(f_\theta(\mathbf{x}_i + \delta_i), y_i)] + \lambda \mathcal{H}(p_{\phi_i}(\delta_i)) \right\}.$$

To solve this, we need to estimate the gradient of the expected loss with respect to the parameters ϕ_i . A commonly used method is the low-variance reparameterization trick (Kingma & Welling, 2014; Blundell et al., 2015), which replaces the sampling process of the random variable of interest with the corresponding differentiable transformation. With this technique, the gradient can be back-propagated from the samples to the distribution parameters directly. In our case, we reparameterize δ_i by $\delta_i = \epsilon \cdot \tanh(\mathbf{u}_i) = \epsilon \cdot \tanh(\mu_i + \sigma_i \mathbf{r})$, where \mathbf{r} is an auxiliary noise variable following the standard Gaussian distribution $\mathcal{N}(\mathbf{0}, \mathbf{I})$. Therefore, we can estimate the gradient of ϕ_i via

$$\mathbb{E}_{\mathbf{r} \sim \mathcal{N}(\mathbf{0}, \mathbf{I})} \nabla_{\phi_i} \left[\mathcal{L}(f_\theta(\mathbf{x}_i + \epsilon \cdot \tanh(\mu_i + \sigma_i \mathbf{r})), y_i) - \lambda \log p_{\phi_i}(\epsilon \cdot \tanh(\mu_i + \sigma_i \mathbf{r})) \right]. \quad (10)$$

The first term inside is the classification loss with the sampled noise, and the second is the negative log density (i.e., estimation of entropy) which can be calculated analytically (proof in Appendix A.2) as

$$\sum_{j=1}^d \left(\frac{1}{2} (\mathbf{r}^{(j)})^2 + \frac{\log 2\pi}{2} + \log \sigma_i^{(j)} + \log (1 - \tanh(\mu_i^{(j)} + \sigma_i^{(j)} \mathbf{r}^{(j)}))^2 + \log \epsilon \right), \quad (11)$$

where the superscript j denotes the j -th element of a vector.

In practice, we approximate the expectation in Eqn. (10) with k Monte Carlo (MC) samples, and perform T steps of gradient ascent on ϕ_i to solve the inner problem. After obtaining the optimal parameters ϕ_i^* , we use the adversarial distribution $p_{\phi_i^*}(\delta_i)$, which characterizes the adversarial perturbations around the natural input \mathbf{x}_i , to update model parameters θ . The algorithm is outlined in Appendix B.1.

3.2. Amortizing the Explicit Adversarial Distributions

Although the aforementioned method in Section 3.1 provides a simple way to learn explicit adversarial distributions for ADT, it needs to learn the distribution parameters for each input and then brings prohibitive computational cost. Compared with the vanilla AT which constructs adversarial examples by T steps PGD (Madry et al., 2018), ADT_{EXP} is approximately k times slower since the gradient of ϕ_i is estimated by k MC samples in each step. In this subsection, we propose to amortize the inner optimization of ADT_{EXP}, to develop a more feasible and scalable training method. We name ADT with the AMortized version of EXPLICIT adversarial distributions as ADT_{EXP-AM}.

Specifically, instead of optimizing the distribution parameters for each data \mathbf{x}_i , we opt to learn a mapping $g_\phi : \mathbb{R}^d \rightarrow \mathcal{P}$, which defines the adversarial distribution for each input in a conditional manner $p_\phi(\delta_i|\mathbf{x}_i)$. We instantiate g_ϕ by a conditional generator network. It takes a natural example \mathbf{x}_i as input, and outputs the parameters (μ_i, σ_i) of its corresponding explicit adversarial distribution which is also defined by Eqn. (9). The notable advantage of using a generator to define $p_\phi(\delta_i|\mathbf{x}_i)$ is that the generator network can potentially learn common structures of the adversarial perturbations, which can generalize to new training samples (Baluja & Fischer, 2017; Poursaeed et al., 2018) with the similar characteristics. It means that we do not need to optimize ϕ excessively on each data \mathbf{x}_i , which can accelerate the training process.

By amortizing the explicit adversarial distributions, we can rewrite the minimax optimization problem (6) as

$$\min_{\theta} \max_{\phi} \frac{1}{n} \sum_{i=1}^n \left\{ \mathbb{E}_{p_\phi(\delta_i|\mathbf{x}_i)} [\mathcal{L}(f_\theta(\mathbf{x}_i + \delta_i), y_i)] + \lambda \mathcal{H}(p_\phi(\delta_i|\mathbf{x}_i)) \right\}, \quad (12)$$

where θ and ϕ are the parameters of the DNN classifier and the generator, respectively. During training, we perform stochastic gradient descent and ascent on θ and ϕ simultaneously, to accomplish adversarial training. To enable the gradients flowing from δ_i to ϕ , we apply the same reparameterization strategy as in Section 3.1. In practice, we only use one MC sample for each data, with the detailed algorithm described in Appendix B.2.

3.3. Implicit Modeling of Adversarial Perturbations

Since the underlying distributions of adversarial perturbations have not been figured out yet and could be different across samples, it is hard to specify a proper explicit distribution to model adversarial perturbations, which may lead to the underfitting issue. To bypass this, we resort to implicit distributions (i.e., distributions without tractable probability density functions but can still be sampled from), which have shown promising results recently (Goodfellow et al., 2014; Shi et al., 2018a;b), particularly in modeling complex high-dimensional data (Radford et al., 2016; Isola et al., 2017). The major advantage of implicit distributions is that they are not confined to provide explicit densities, which intrinsically improve the flexibility inside the sampling process.

Based on this analysis, we propose to use the implicit distributions to characterize the adversarial perturbations of each data \mathbf{x}_i . Considering the priority of amortized optimization, we learn a generator $g_\phi : \mathbb{R}^{d_z} \times \mathbb{R}^d \rightarrow \mathbb{R}^d$ which implicitly defines a conditional distribution $p_\phi(\delta_i|\mathbf{x}_i)$ by

$$\delta_i = g_\phi(\mathbf{z}; \mathbf{x}_i), \quad (13)$$

where \mathbf{x}_i is a natural input and $\mathbf{z} \in \mathbb{R}^{d_z}$ is a random noise vector. Typically, \mathbf{z} is sampled from a general prior $p(\mathbf{z})$ such as the standard Gaussian or uniform distributions as in the generative adversarial networks (GANs) (Goodfellow et al., 2014). In this work, we sample \mathbf{z} from a uniform distribution $U(-1, 1)$. We refer to this approach as ADT_{IMP-AM}.

A practical problem remains untackled is that the entropy of the implicit distributions cannot be estimated exactly as we have no access to the density $p_\phi(\delta_i|\mathbf{x}_i)$. This leads to the failure of naive optimization. An appealing alternative is to maximize the variational lower bound of the entropy (Dai et al., 2017a)² for its simplicity and success in GANs (Dai et al., 2017b). In our case, for a natural input \mathbf{x}_i , we can similarly derive the following lower bound stemming from the mutual information between the perturbation δ_i and the random noise \mathbf{z} (proof in Appendix A.3) as

$$\mathcal{H}(p_\phi(\delta_i|\mathbf{x}_i)) \geq \mathcal{U}(q) = \mathbb{E}_{p(\mathbf{z})} \log q(\mathbf{z}|g_\phi(\mathbf{z}; \mathbf{x}_i)) + c, \quad (14)$$

where c is a constant and $q(\cdot|\cdot)$ is an introduced variational distribution. Maximizing $\mathcal{U}(q)$ can effectively maximize the entropy term $\mathcal{H}(p_\phi(\delta_i|\mathbf{x}_i))$. In practice, we implement q as a diagonal Gaussian, whose mean and standard derivation are given by a ψ -parameterized neural network. Then we have the final training objective as

$$\min_{\theta} \max_{\phi, \psi} \frac{1}{n} \sum_{i=1}^n \left\{ \mathbb{E}_{p(\mathbf{z})} [\mathcal{L}(f_\theta(\mathbf{x}_i + g_\phi(\mathbf{z}; \mathbf{x}_i)), y_i)] + \lambda \log q_\psi(\mathbf{z}|g_\phi(\mathbf{z}; \mathbf{x}_i)) \right\}, \quad (15)$$

²We can also directly estimate the gradient of the entropy with advanced techniques such as spectral Stein gradient estimator (Shi et al., 2018b), and we leave this for future work.

which is solved by simultaneous stochastic gradient descent and ascent on θ and (ϕ, ψ) . We also provide the detailed training algorithm of ADT_{IMP-AM} in Appendix B.3.

4. Related Work

Our work is related to some previous work in the literature. Learning the distributions of adversarial examples has been studied before, mainly for black-box adversarial attacks. In Ilyas et al. (2018), an adversarial example is searched over a distribution, similar to the inner problem of Eqn. (4). They use natural evolution strategy to estimate the gradient for black-box attacks. But their gradient estimator exhibits very high variance compared with ours in Eqn. (10) (Kingma & Welling, 2014). And our method is based on the white-box setting (i.e., compute the gradient) rather than the black-box setting. Li et al. (2019) further improve the query-efficiency of black-box attacks by learning the distribution parameters. To the best of our knowledge, we are the first to train robust models by learning the adversarial distributions.

In this work, we adopt a generator network to amortize the adversarial distributions for accelerating the training process. There also exists previous work on using generator-based approaches for adversarial attacks and defenses (Baluja & Fischer, 2017; Poursaeed et al., 2018; Xiao et al., 2018). Wang & Yu (2019) and Chen et al. (2018) propose to solve the inner maximization problem of AT by generating adversarial examples using a generator network, which are similar to our work. The essential difference is that they still focus on the minimax formulation (1) of AT, while we propose a novel ADT framework in Eqn. (4). We empirically compare our method with Chen et al. (2018) in Appendix D.4.

The proposed ADT framework is essentially different from a seemingly similar concept, called distributionally robust optimization (DRO) (Ben-Tal et al., 2013; Esfahani & Kuhn, 2018; Sinha et al., 2018). DRO seeks a model that is robust against changes in data-generating distribution, by training on the worst-case data distribution under a probability measure. DRO is related to AT with the Wasserstein distance (Sinha et al., 2018; Staib & Jegelka, 2017). However, ADT does not model the changes in data distribution but aims to find an adversarial distribution for each input.

5. Experiments

To empirically validate the effectiveness of ADT on improving the adversarial robustness of DNNs, we perform extensive experiments on several benchmark datasets. All of the experiments are conducted on NVIDIA 2080 Ti GPUs.

5.1. Experimental Settings and Implementation Details

We briefly introduce the experimental settings in this section, and leave the full details in Appendix C.

Datasets. We choose CIFAR-10, CIFAR-100 (Krizhevsky & Hinton, 2009), and SVHN (Netzer et al., 2011) to conduct experiments. The images are normalized to $[0, 1]$. We set the perturbation budget $\epsilon = 8/255$ on CIFAR, and $\epsilon = 4/255$ on SVHN, as in Carmon et al. (2019).

Network Architectures. We use a Wide ResNet (WRN-28-10) model (Zagoruyko & Komodakis, 2016) as the classifier in all of our experiments, following Madry et al. (2018). For the generator network used in ADT_{EXP-AM} and ADT_{IMP-AM}, we adopt a popular image-to-image architecture with residual blocks (Johnson et al., 2016; Zhu et al., 2017). We also employ a 5-layer CNN to instantiate q_ψ in ADT_{IMP-AM}.

Training Details. We adopt the cross-entropy loss as \mathcal{L} in our objective (6). We set $\lambda = 0.01$ for the entropy term, and leave the study of the effects of λ in Section 5.4. For ADT_{EXP}, we adopt Adam (Kingma & Ba, 2015) for optimizing ϕ_i with the learning rate 0.3, the optimization steps $T = 7$, and the number of MC samples in each step $k = 5$. For ADT_{EXP-AM} and ADT_{IMP-AM}, we adopt Adam with only one MC sample for each data for gradient estimation.

Baselines. We compare the effectiveness of ADT with two primary and representative baselines: 1) standard training on the natural images (**Standard**); 2) AT on the PGD adversarial examples (**AT_{PGD}**) (Madry et al., 2018). We also include the pretrained AT_{PGD} model released by Madry et al. (2018), which is denoted as **AT_{PGD}[†]**. On CIFAR-10, we further incorporate several additional baselines for comprehensive evaluations, including: 1) AT on the targeted FGSM adversarial examples (**AT_{FGSM}**) (Kurakin et al., 2017); 2) adversarial logit pairing (**ALP**) (Kannan et al., 2018); and 3) feature scattering-based AT (**FeaScatter**) (Zhang & Wang, 2019). We additionally compare with Zhang et al. (2019) and Chen et al. (2018) in Appendix D.3 and D.4.

Robustness Evaluation. To evaluate the adversarial robustness of these models, we adopt a plenty of attack methods, and report the *per-example accuracy* as suggested in Carlini et al. (2019), which calculates the robust accuracy by

$$\mathcal{A}_{\text{rob}} = \frac{1}{n_{\text{test}}} \sum_{i=1}^{n_{\text{test}}} \min_{a \in \mathbf{A}} \mathbb{I}(\arg \max\{f_\theta(a(\mathbf{x}_i))\} = y_i),$$

where \mathbf{A} is the set of tested attacks, $a(\mathbf{x}_i)$ is the adversarial example given by attack a , and $\mathbb{I}(\cdot)$ is the indicator function.

5.2. Robustness under White-box Attacks

We first compare the robustness of the proposed methods with baselines under various white-box attacks. We consider FGSM (Goodfellow et al., 2015), PGD (Madry et al., 2018), MIM (Dong et al., 2018), C&W (Carlini & Wagner, 2017), and a feature attack (FeaAttack)³ for evaluation. C&W is

³<https://github.com/Line290/FeatureAttack>.

Table 1. Classification accuracy of the three proposed methods and baselines on CIFAR-10 under white-box attacks with $\epsilon = 8/255$. The last column shows the overall robustness of the models. We mark the best results for each attack and the overall results that outperform the baselines in **bold**, and the overall best result in **blue**. We highlight the results of AT_{FGSM} and FeaScatter in **orange** to emphasize that these models have the generalization problem across attacks, whose overall robustness is weak.

Model	\mathcal{A}_{nat}	FGSM	PGD-20	PGD-100	MIM	C&W	FeaAttack	\mathcal{A}_{rob}
Standard	94.81%	12.05%	0.00%	0.00%	0.00%	0.00%	0.00%	0.00%
AT_{FGSM}	93.80%	79.86%	0.12%	0.04%	0.06%	0.13%	0.01%	0.01%
$\text{AT}_{\text{PGD}}^{\dagger}$	87.25%	56.04%	45.88%	45.33%	47.15%	46.67%	46.01%	44.89%
AT_{PGD}	86.91%	58.30%	50.03%	49.40%	51.40%	50.23%	50.46%	48.26%
ALP	86.81%	56.83%	48.97%	48.60%	50.13%	49.10%	48.51%	47.90%
FeaScatter	89.98%	77.40%	70.85%	68.81%	72.74%	58.46%	37.45%	37.40%
ADT_{EXP}	86.89%	60.41%	52.18%	51.69%	53.27%	52.49%	52.38%	50.56%
$\text{ADT}_{\text{EXP-AM}}$	87.82%	62.42%	51.95%	51.26%	52.99%	51.75%	52.04%	50.04%
$\text{ADT}_{\text{IMP-AM}}$	88.00%	64.89%	52.28%	51.23%	52.64%	52.65%	51.89%	49.81%

Table 2. Classification accuracy of the three proposed methods and baselines on CIFAR-100 and SVHN under white-box attacks. We mark the best results for each attack and the overall results that outperform the baselines in **bold**, and the overall best result in **blue**.

Model	\mathcal{A}_{nat}	FGSM	PGD-20	PGD-100	MIM	C&W	FeaAttack	\mathcal{A}_{rob}
CIFAR100, $\epsilon = 8/255$								
Standard	78.59%	8.73%	0.02%	0.01%	0.02%	0.00%	0.00%	0.00%
AT_{PGD}	61.45%	30.78%	25.71%	25.40%	26.60%	25.80%	33.95%	24.49%
ADT_{EXP}	62.70%	34.22%	28.96%	28.60%	29.83%	28.99%	35.07%	27.13%
$\text{ADT}_{\text{EXP-AM}}$	62.84%	36.28%	29.01%	28.46%	29.68%	28.78%	34.91%	26.87%
$\text{ADT}_{\text{IMP-AM}}$	64.07%	39.39%	29.40%	28.43%	29.64%	28.76%	35.00%	26.80%
SVHN, $\epsilon = 4/255$								
Standard	96.12%	39.05%	3.64%	2.95%	4.08%	3.91%	2.14%	2.14%
AT_{PGD}	95.07%	82.19%	74.22%	73.79%	74.56%	74.77%	73.51%	73.38%
ADT_{EXP}	95.70%	86.72%	77.01%	76.62%	77.18%	77.50%	75.64%	75.55%
$\text{ADT}_{\text{EXP-AM}}$	95.67%	85.24%	76.12%	75.58%	76.63%	76.70%	75.20%	75.00%
$\text{ADT}_{\text{IMP-AM}}$	95.62%	86.73%	75.61%	74.85%	75.91%	76.12%	74.24%	74.13%

implemented by adopting the margin-based loss function in Carlini & Wagner (2017) and using PGD for optimization. We use 20 and 100 steps for PGD, 20 steps for MIM, and 30 steps for C&W. The step size is $\alpha = \epsilon/4$ in these attacks. FeaAttack is a stronger attack for the defense FeaScatter. The details of FeaAttack are provided in Appendix C.5.

On **CIFAR-10**, we compare the classification accuracy of the proposed methods— ADT_{EXP} , $\text{ADT}_{\text{EXP-AM}}$, $\text{ADT}_{\text{IMP-AM}}$, and baseline models—Standard, AT_{FGSM} , AT_{PGD} , $\text{AT}_{\text{PGD}}^{\dagger}$, ALP, FeaScatter on natural inputs and adversarial examples in Table 1. It is obvious that some AT-based methods exhibit the generalization problem across attacks, i.e., AT_{FGSM} and FeaScatter, whose overall robustness is weak. But ADT-based methods do not have this issue by showing consistent robustness performance across all tested attacks. Although AT_{PGD} does not have this issue also, and achieves the best performance among the AT-based defenses, the proposed ADT reveals improved overall robustness than AT_{PGD} , showing the effectiveness of the proposed methods. We also show the results on **CIFAR-100** and **SVHN** in Table 2. The results consistently demonstrate that ADT-based methods can outperform AT_{PGD} under white-box attacks.

It can be further seen that ADT_{EXP} is better than $\text{ADT}_{\text{EXP-AM}}$ and $\text{ADT}_{\text{IMP-AM}}$ in most cases. We suspect the reason is that amortizing the adversarial distributions through a generator network is hard to deliver appropriate adversarial regions

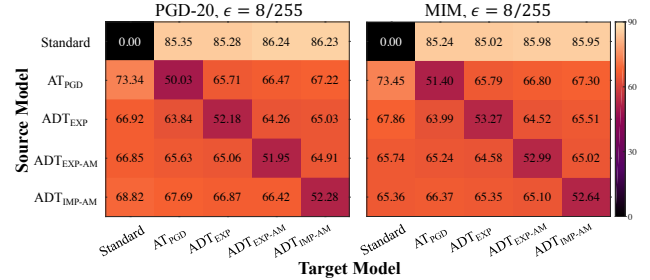


Figure 2. Classification accuracy (%) of the three proposed methods and baselines on CIFAR-10 under transfer-based black-box attacks. The *source model* refers to the one used to craft adversarial examples, and the *target model* is the one being attacked.

for every input, owing to the limited capacity of the generator. Nevertheless, it can accelerate the training, which is shown in Appendix D.2. Note that $\text{ADT}_{\text{IMP-AM}}$ obtains similar robustness with $\text{ADT}_{\text{EXP-AM}}$. It indicates that though the adopted implicit distributions enable us to optimize in a larger distribution family and the optimization always converges to local optima, learning in $\text{ADT}_{\text{IMP-AM}}$ does not necessarily lead to better adversarial distributions and more robust models.

5.3. Robustness under Black-box Attacks

Now we evaluate the robustness of the defenses on CIFAR-10 under black-box attacks to perform a thorough evaluation following the guidelines in Carlini et al. (2019). We first

Table 3. Classification accuracy of the three proposed methods and baselines on CIFAR-10 under the black-box SPSA attack with different batch sizes. The perturbation budget is $\epsilon = 8/255$.

Model	SPSA			
	256	512	1024	2048
Standard	0.00%	0.00%	0.00%	0.00%
AT _{PGD}	56.60%	53.50%	50.62%	47.83%
ADT _{EXP}	58.67%	55.39%	52.67%	50.42%
ADT _{EXP-AM}	58.67%	55.02%	52.30%	49.57%
ADT _{IMP-AM}	58.58%	55.23%	52.19%	49.39%

evaluate *transfer-based black-box attacks* using PGD-20 and MIM. The results in Figure 2 show that these models obtain higher accuracy under transfer-based attacks than white-box attacks. We further perform *query-based black-box attacks* using SPSA (Uesato et al., 2018) and report the results in Table 3. To estimate the gradients, we set the batch size as 256, 512, 1024, and 2048, the perturbation size as 0.001, and the learning rate as 0.01. We run SPSA attacks for a maximum of 100 iterations, and stop when we cause misclassification. The results also show that the accuracy is higher than that under white-box attacks. And our methods obtain better robustness compared with AT_{PGD}. In summary, the results under black-box attacks verify that our methods can reliably improve the robustness rather than causing gradient masking (Athalye et al., 2018).

5.4. Additional Results and Ablation Studies

Attack Performance of Adversarial Distributions. First, we explore the attack performance of the three proposed methods (i.e., EXP, EXP-AM, and IMP-AM) for learning the adversarial distributions. We choose Standard, AT_{PGD}, ADT_{EXP}, ADT_{EXP-AM}, and ADT_{IMP-AM} as the target models. For EXP, we set the optimization steps as $T = 20$, the number of MC samples in each step as $k = 10$ to conduct a more powerful attack. We further study the convergence of EXP in Appendix D.1. For EXP-AM and IMP-AM, we retrain the generator networks for each pretrained defense. The classification results are shown in Table 4. From the results, EXP is slightly stronger than PGD-20 while EXP-AM and IMP-AM exhibit comparable attack power.

Table 4. Classification Accuracy of the three proposed methods and baselines on CIFAR-10 under PGD-20, EXP, EXP-AM, and IMP-AM attacks with $\epsilon = 8/255$.

Model	PGD-20	EXP	EXP-AM	IMP-AM
Standard	0.00%	0.00%	9.24%	9.83%
AT _{PGD}	50.03%	49.97%	50.46%	50.36%
ADT _{EXP}	52.18%	51.96%	52.71%	52.82%
ADT _{EXP-AM}	51.95%	51.62%	52.85%	52.72%
ADT _{IMP-AM}	52.28%	51.46%	52.76%	52.48%

The Impact of λ . We study the impact of λ on the performance of ADT. We choose ADT_{EXP-AM} as a case study for its fast training process and analytical entropy estimation. Figure 3 shows the robustness under white-box attacks

and the average entropy of the adversarial distributions of ADT_{EXP-AM} trained with $\lambda = 0.0, 0.001, 0.01, 0.1$, and 1.0. Generally, a larger λ leads to a larger entropy and better robustness. But a too large λ will reduce the robustness.

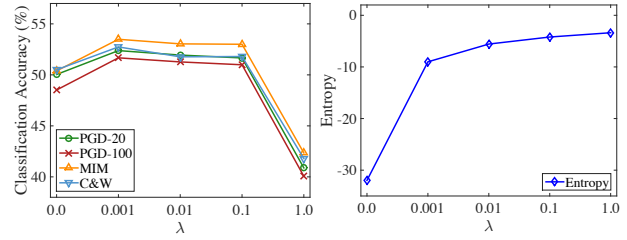


Figure 3. Classification accuracy (%) under white-box attacks and the average entropy of the adversarial distributions of ADT_{EXP-AM} on CIFAR-10 trained with $\lambda = 0.0, 0.001, 0.01, 0.1$, and 1.0.

Loss Landscape Analysis. We conduct an additional check against gradient masking (Athalye et al., 2018) by looking at the loss landscape. First, we plot the cross-entropy loss of the models projected along the gradient direction (\mathbf{d}_g) and a random direction (\mathbf{d}_r) in the vicinity of a natural input in Figure 4. Notably, the models trained by ADT exhibit smoother and more flattened loss surfaces than Standard and AT_{PGD}, and thus deliver better robustness. We further quantitatively measure the smoothness of loss surfaces with the dominant eigenvalue of the Hessian matrix of the classification loss with respect to the input as a proxy. We use 1,000 images from the test set of CIFAR-10 for calculation, and report the mean and standard derivation in Figure 4(f). The numbers are consistent with the visualization results and help us confirm the superiority of ADT upon AT to learn smooth loss surfaces and robust deep models.

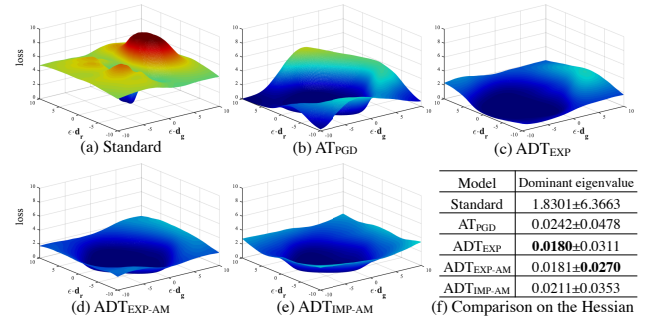


Figure 4. Visualization of loss surfaces in the vicinity of a natural input along the gradient direction (\mathbf{d}_g) and a random (Rademacher) direction (\mathbf{d}_r) for the trained models in (a)-(e). We also report the dominant eigenvalue of the Hessian matrix of the classification loss with respect to the input in (f) for a quantitative comparison.

6. Conclusion

In this paper, we introduced an adversarial distributional training framework for learning robust DNNs. We proposed to parameterize the adversarial distributions in ADT with three different approaches. The experiments demonstrate the effectiveness of ADT on building robust DNNs, compared with the state-of-the-art adversarial training methods.

References

- Alayrac, J.-B., Uesato, J., Huang, P.-S., Fawzi, A., Stanforth, R., and Kohli, P. Are labels required for improving adversarial robustness? In *Advances in Neural Information Processing Systems (NeurIPS)*, 2019.
- Athalye, A., Carlini, N., and Wagner, D. Obfuscated gradients give a false sense of security: Circumventing defenses to adversarial examples. In *International Conference on Machine Learning (ICML)*, 2018.
- Baluja, S. and Fischer, I. Adversarial transformation networks: Learning to generate adversarial examples. *arXiv preprint arXiv:1703.09387*, 2017.
- Ben-Tal, A., Den Hertog, D., De Waegenare, A., Melenberg, B., and Rennen, G. Robust solutions of optimization problems affected by uncertain probabilities. *Management Science*, 59(2):341–357, 2013.
- Blundell, C., Cornebise, J., Kavukcuoglu, K., and Wierstra, D. Weight uncertainty in neural networks. In *International Conference on Machine Learning (ICML)*, 2015.
- Carlini, N. and Wagner, D. Towards evaluating the robustness of neural networks. In *IEEE Symposium on Security and Privacy*, 2017.
- Carlini, N., Athalye, A., Papernot, N., Brendel, W., Rauber, J., Tsipras, D., Goodfellow, I., and Madry, A. On evaluating adversarial robustness. *arXiv preprint arXiv:1902.06705*, 2019.
- Carmon, Y., Ragunathan, A., Schmidt, L., Liang, P., and Duchi, J. C. Unlabeled data improves adversarial robustness. In *Advances in Neural Information Processing Systems (NeurIPS)*, 2019.
- Chen, Z., Jiang, H., Shi, Y., Dai, B., and Zhao, T. Learning to defense by learning to attack. *arXiv preprint arXiv:1811.01213*, 2018.
- Dai, Z., Almahairi, A., Bachman, P., Hovy, E., and Courville, A. Calibrating energy-based generative adversarial networks. In *International Conference on Learning Representations (ICLR)*, 2017a.
- Dai, Z., Yang, Z., Yang, F., Cohen, W. W., and Salakhutdinov, R. R. Good semi-supervised learning that requires a bad gan. In *Advances in Neural Information Processing Systems (NeurIPS)*, 2017b.
- Danskin, J. M. *The theory of max-min and its application to weapons allocation problems*, volume 5. Springer Science & Business Media, 2012.
- Devlin, J., Chang, M.-W., Lee, K., and Toutanova, K. Bert: Pre-training of deep bidirectional transformers for language understanding. In *Proceedings of the 2019 Conference of the North American Chapter of the Association for Computational Linguistics: Human Language Technologies (NAACL-HLT)*, 2019.
- Dong, Y., Liao, F., Pang, T., Su, H., Zhu, J., Hu, X., and Li, J. Boosting adversarial attacks with momentum. In *Proceedings of the IEEE Conference on Computer Vision and Pattern Recognition (CVPR)*, 2018.
- Engstrom, L., Tran, B., Tsipras, D., Schmidt, L., and Madry, A. Exploring the landscape of spatial robustness. In *International Conference on Machine Learning (ICML)*, 2019.
- Esfahani, P. M. and Kuhn, D. Data-driven distributionally robust optimization using the wasserstein metric: Performance guarantees and tractable reformulations. *Mathematical Programming*, 171(1-2):115–166, 2018.
- Goodfellow, I., Pouget-Abadie, J., Mirza, M., Xu, B., Warde-Farley, D., Ozair, S., Courville, A., and Bengio, Y. Generative adversarial nets. In *Advances in Neural Information Processing Systems (NeurIPS)*, 2014.
- Goodfellow, I. J., Shlens, J., and Szegedy, C. Explaining and harnessing adversarial examples. In *International Conference on Learning Representations (ICLR)*, 2015.
- Graves, A., Mohamed, A. R., and Hinton, G. Speech recognition with deep recurrent neural networks. In *IEEE International Conference on Acoustics, Speech and Signal Processing*, pp. 6645–6649, 2013.
- He, K., Zhang, X., Ren, S., and Sun, J. Deep residual learning for image recognition. In *Proceedings of the IEEE Conference on Computer Vision and Pattern Recognition (CVPR)*, 2016.
- Hendrycks, D. and Dietterich, T. Benchmarking neural network robustness to common corruptions and perturbations. In *International Conference on Learning Representations (ICLR)*, 2019.
- Hendrycks, D., Lee, K., and Mazeika, M. Using pre-training can improve model robustness and uncertainty. In *International Conference on Machine Learning (ICML)*, 2019.
- Ilyas, A., Engstrom, L., Athalye, A., and Lin, J. Black-box adversarial attacks with limited queries and information. In *International Conference on Machine Learning (ICML)*, 2018.
- Ioffe, S. and Szegedy, C. Batch normalization: Accelerating deep network training by reducing internal covariate shift. In *International Conference on Machine Learning (ICML)*, 2015.

- Isola, P., Zhu, J.-Y., Zhou, T., and Efros, A. A. Image-to-image translation with conditional adversarial networks. In *Proceedings of the IEEE conference on computer vision and pattern recognition (CVPR)*, 2017.
- Johnson, J., Alahi, A., and Fei-Fei, L. Perceptual losses for real-time style transfer and super-resolution. In *European Conference on Computer Vision (ECCV)*, 2016.
- Kannan, H., Kurakin, A., and Goodfellow, I. Adversarial logit pairing. *arXiv preprint arXiv:1803.06373*, 2018.
- Kingma, D. and Ba, J. Adam: A method for stochastic optimization. In *International Conference on Learning Representations (ICLR)*, 2015.
- Kingma, D. P. and Welling, M. Auto-encoding variational bayes. In *International Conference on Learning Representations (ICLR)*, 2014.
- Krizhevsky, A. and Hinton, G. Learning multiple layers of features from tiny images. Technical report, University of Toronto, 2009.
- Krizhevsky, A., Sutskever, I., and Hinton, G. E. Imagenet classification with deep convolutional neural networks. In *Advances in Neural Information Processing Systems (NeurIPS)*, 2012.
- Kurakin, A., Goodfellow, I., and Bengio, S. Adversarial machine learning at scale. In *International Conference on Learning Representations (ICLR)*, 2017.
- Li, Y., Li, L., Wang, L., Zhang, T., and Gong, B. Nattack: Learning the distributions of adversarial examples for an improved black-box attack on deep neural networks. In *International Conference on Machine Learning (ICML)*, 2019.
- Liao, F., Liang, M., Dong, Y., Pang, T., Hu, X., and Zhu, J. Defense against adversarial attacks using high-level representation guided denoiser. In *Proceedings of the IEEE Conference on Computer Vision and Pattern Recognition (CVPR)*, 2018.
- Louizos, C. and Welling, M. Structured and efficient variational deep learning with matrix gaussian posteriors. In *International Conference on Machine Learning (ICML)*, 2016.
- Louizos, C. and Welling, M. Multiplicative normalizing flows for variational bayesian neural networks. In *International Conference on Machine Learning (ICML)*, 2017.
- Madry, A., Makelov, A., Schmidt, L., Tsipras, D., and Vladu, A. Towards deep learning models resistant to adversarial attacks. In *International Conference on Learning Representations (ICLR)*, 2018.
- Netzer, Y., Wang, T., Coates, A., Bissacco, A., Wu, B., and Ng, A. Y. Reading digits in natural images with unsupervised feature learning. In *NIPS Workshop on Deep Learning and Unsupervised Feature Learning*, 2011.
- Pang, T., Xu, K., Du, C., Chen, N., and Zhu, J. Improving adversarial robustness via promoting ensemble diversity. In *International Conference on Machine Learning (ICML)*, 2019.
- Papernot, N., McDaniel, P., Wu, X., Jha, S., and Swami, A. Distillation as a defense to adversarial perturbations against deep neural networks. In *IEEE Symposium on Security and Privacy*, 2016.
- Poursaeed, O., Katsman, I., Gao, B., and Belongie, S. Generative adversarial perturbations. In *Proceedings of the IEEE Conference on Computer Vision and Pattern Recognition (CVPR)*, 2018.
- Radford, A., Metz, L., and Chintala, S. Unsupervised representation learning with deep convolutional generative adversarial networks. In *International Conference on Learning Representations (ICLR)*, 2016.
- Shi, J., Sun, S., and Zhu, J. Kernel implicit variational inference. In *International Conference on Learning Representations (ICLR)*, 2018a.
- Shi, J., Sun, S., and Zhu, J. A spectral approach to gradient estimation for implicit distributions. In *International Conference on Machine Learning (ICML)*, 2018b.
- Sinha, A., Namkoong, H., and Duchi, J. Certifying some distributional robustness with principled adversarial training. In *International Conference on Learning Representations (ICLR)*, 2018.
- Song, C., He, K., Wang, L., and Hopcroft, J. E. Improving the generalization of adversarial training with domain adaptation. In *International Conference on Learning Representations (ICLR)*, 2019.
- Staib, M. and Jegelka, S. Distributionally robust deep learning as a generalization of adversarial training. In *NIPS workshop on Machine Learning and Computer Security*, 2017.
- Szegedy, C., Zaremba, W., Sutskever, I., Bruna, J., Erhan, D., Goodfellow, I., and Fergus, R. Intriguing properties of neural networks. In *International Conference on Learning Representations (ICLR)*, 2014.
- Tramèr, F. and Boneh, D. Adversarial training and robustness for multiple perturbations. In *Advances in Neural Information Processing Systems (NeurIPS)*, 2019.

- Tramèr, F., Kurakin, A., Papernot, N., Boneh, D., and McDaniel, P. Ensemble adversarial training: Attacks and defenses. In *International Conference on Learning Representations (ICLR)*, 2018.
- Uesato, J., O’Donoghue, B., Oord, A. v. d., and Kohli, P. Adversarial risk and the dangers of evaluating against weak attacks. In *International Conference on Machine Learning (ICML)*, 2018.
- Wang, H. and Yu, C.-N. A direct approach to robust deep learning using adversarial networks. In *International Conference on Learning Representations (ICLR)*, 2019.
- Wong, E. and Kolter, Z. Provable defenses against adversarial examples via the convex outer adversarial polytope. In *International Conference on Machine Learning (ICML)*, 2018.
- Wong, E., Rice, L., and Kolter, J. Z. Fast is better than free: Revisiting adversarial training. In *International Conference on Learning Representations (ICLR)*, 2020.
- Xiao, C., Li, B., Zhu, J.-Y., He, W., Liu, M., and Song, D. Generating adversarial examples with adversarial networks. In *International Joint Conference on Artificial Intelligence (IJCAI)*, 2018.
- Zagoruyko, S. and Komodakis, N. Wide residual networks. In *Proceedings of the British Machine Vision Conference (BMVC)*, 2016.
- Zhang, H. and Wang, J. Defense against adversarial attacks using feature scattering-based adversarial training. In *Advances in Neural Information Processing Systems (NeurIPS)*, 2019.
- Zhang, H., Yu, Y., Jiao, J., Xing, E. P., Ghaoui, L. E., and Jordan, M. I. Theoretically principled trade-off between robustness and accuracy. In *International Conference on Machine Learning (ICML)*, 2019.
- Zhu, J.-Y., Park, T., Isola, P., and Efros, A. A. Unpaired image-to-image translation using cycle-consistent adversarial networks. In *Proceedings of the IEEE International Conference on Computer Vision (ICCV)*, 2017.

A. Proofs

We provide the proofs in this section.

A.1. Proof of Theorem 1

Assumption 1. The loss function $\mathcal{J}(p(\delta_i), \theta)$ is continuously differentiable with respect to θ .

Assumption 2. The probability density functions of distributions in \mathcal{P} are bounded and equicontinuous.

Remark 1. For the explicit adversarial distributions defined in Eqn. (9), we can assume that the mean and standard deviation of each dimension satisfy $|\mu_i^{(j)}| < \kappa_\mu$ and $\kappa_\sigma^{lo} < \sigma_i^{(j)} < \kappa_\sigma^{up}$, where κ_μ , κ_σ^{lo} , and κ_σ^{up} are constants. Note that they can be easily satisfied since we add an entropic regularization term into the training objective (6), such that the mean cannot be too large while the standard deviation cannot be too small or too large given Eqn. (11). In practice, we can clip $\mu_i^{(j)}$ and $\sigma_i^{(j)}$ if they are out of the thresholds. Then we can prove that the density functions of the explicit adversarial distributions defined in Eqn. (9) are bounded and equicontinuous, satisfying Assumption 2. However, for the implicit adversarial distributions introduced in Section 3.3, we cannot prove that Assumption 2 is satisfied. Though unsatisfied, the experiments suggest that we can still rely on Theorem 1 and the general algorithm for training.

Proof. Due to the diagonal covariance matrix, each dimension of $p_{\phi_i}(\delta_i)$ is independent. Thus we only consider one dimension of δ_i . For clarity, we denote $\mu_i^{(j)}$, $\sigma_i^{(j)}$, $\mathbf{r}^{(j)}$, $\mathbf{u}_i^{(j)}$, and $\delta_i^{(j)}$ as μ , σ , r , u , and δ , respectively. The probability density function of δ is (see Appendix A.2 for details)

$$\begin{aligned} p(\delta) &= \frac{1}{\sqrt{2\pi}\sigma} \exp\left(-\frac{(\frac{1}{2} \log \frac{\epsilon+\delta}{\epsilon-\delta} - \mu)^2}{2\sigma^2}\right) \cdot \frac{\epsilon}{\epsilon^2 - \delta^2} \\ &= \frac{1}{\sqrt{2\pi}\sigma} \exp\left(-\frac{r^2}{2}\right) \cdot \frac{1}{1 - \tanh(\mu + \sigma r)^2} \cdot \frac{1}{\epsilon}. \end{aligned}$$

By calculation, we have

$$\begin{aligned} p(\delta) &= \frac{1}{4\sqrt{2\pi}\sigma\epsilon} \left[\exp\left(-\frac{r^2}{2} + 2\sigma r + 2\mu\right) \right. \\ &\quad \left. + 2 \exp\left(-\frac{r^2}{2}\right) + \exp\left(-\frac{r^2}{2} - 2\sigma r - 2\mu\right) \right] \\ &\leq \frac{1}{4\sqrt{2\pi}\sigma\epsilon} \left[\exp(2\sigma^2 + 2\mu) + 2 + \exp(2\sigma^2 - 2\mu) \right] \\ &\leq \frac{1}{4\sqrt{2\pi}\kappa_\sigma^{lo}\epsilon} \left[2 \exp(2(\kappa_\sigma^{up})^2) + 2\kappa_\mu + 2 \right]. \end{aligned}$$

Hence, $p(\delta)$ is bounded. And the probability density function $p_{\phi_i}(\delta_i)$ is also bounded since it equals to the product of $p(\delta)$ across all dimensions.

We next prove $p(\delta)$ is Lipschitz continuous at $\delta \in (-\epsilon, \epsilon)$. By calculating the derivative of $p(\delta)$, we have

$$\begin{aligned} p'(\delta) &= \frac{1}{\sqrt{2\pi}\sigma} \exp\left(-\frac{(\frac{1}{2} \log \frac{\epsilon+\delta}{\epsilon-\delta} - \mu)^2}{2\sigma^2}\right) \cdot \left[\frac{2\epsilon\delta}{(\epsilon^2 - \delta^2)^2} \right. \\ &\quad \left. + \frac{\frac{1}{2} \log \frac{\epsilon+\delta}{\epsilon-\delta} - \mu}{\sigma^2} \cdot \left(\frac{\epsilon}{\epsilon^2 - \delta^2}\right)^2 \right] \\ &= \frac{1}{\sqrt{2\pi}\sigma} \exp\left(-\frac{r^2}{2}\right) \cdot \left[\frac{2 \tanh(\mu + \sigma r)}{\epsilon^2(1 - \tanh(\mu + \sigma r)^2)^2} \right. \\ &\quad \left. + \frac{r}{\sigma\epsilon^2(1 - \tanh(\mu + \sigma r)^2)^2} \right]. \end{aligned}$$

Note that although $p'(\delta)$ has a more complicated form, the quadratic term inside \exp is still $-\frac{r^2}{2}$. Hence, $p'(\delta)$ can also be bounded by a constant. Then $p(\delta)$ as well as $p_{\phi_i}(\delta_i)$ are Lipschitz continuous. The Lipschitz constant only concerns with ϵ , κ_μ , κ_σ^{lo} , and κ_σ^{up} . Hence, the set of explicit distributions in \mathcal{P} with a common Lipschitz constant is equicontinuous.

Combining the results, we prove that the probability density functions of the set of explicit adversarial distributions defined in Eqn. (9) are bound and equicontinuous, which satisfies Assumption 2. \square

Theorem 1. Suppose Assumptions 1 and 2 hold. We define $\rho(\theta) = \max_{p(\delta_i) \in \mathcal{P}} \mathcal{J}(p(\delta_i), \theta)$, and $\mathcal{P}^*(\theta) = \{p(\delta_i) \in \mathcal{P} : \mathcal{J}(p(\delta_i), \theta) = \rho(\theta)\}$. Then $\rho(\theta)$ is directionally differentiable, and its directional derivative along the direction \mathbf{v} satisfies

$$\rho'(\theta; \mathbf{v}) = \sup_{p(\delta_i) \in \mathcal{P}^*(\theta)} \mathbf{v}^\top \nabla_{\theta} \mathcal{J}(p(\delta_i), \theta).$$

In particular, when the set $\mathcal{P}^*(\theta) = \{p^*(\delta_i)\}$ only contains one maximizer, $\rho(\theta)$ is differentiable at θ and

$$\nabla_{\theta} \rho(\theta) = \nabla_{\theta} \mathcal{J}(p^*(\delta_i), \theta).$$

Proof. Recall that \mathcal{P} is a set of distributions, which can be expressed by their probability density functions. The support of these functions is contained in \mathcal{S} and these functions are equicontinuous by Assumption 2. $\mathcal{S} = \{\delta : \|\delta\|_\infty \leq \epsilon\}$ is the allowed perturbation set. The Euclidean distance ℓ_2 defines a metric on \mathcal{S} . We let

$$\mathcal{C}(\mathcal{S}, \mathbb{R}) = \{h : \mathcal{S} \rightarrow \mathbb{R} | h \text{ is continuous}\}$$

be the collection of all continuous functions from \mathcal{S} to \mathbb{R} . Then \mathcal{P} is a subset of $\mathcal{C}(\mathcal{S}, \mathbb{R})$. We let

$$d_{\mathcal{C}}(p, q) = \max_{\delta \in \mathcal{S}} |p(\delta) - q(\delta)|$$

for all $p, q \in \mathcal{C}(\mathcal{S}, \mathbb{R})$ be a metric on $\mathcal{C}(\mathcal{S}, \mathbb{R})$. Then we can see that $(\mathcal{C}(\mathcal{S}, \mathbb{R}), d_{\mathcal{C}})$ is a metric space.

We state the following lemma to prove that \mathcal{P} is compact.

Lemma 1. (Arzelà-Ascoli's Theorem) Let (X, d_X) be a compact metric space. A subset \mathcal{K} of $\mathcal{C}(X, \mathbb{R})$ is compact if and only if it is closed, bounded, and equicontinuous.

Since (\mathcal{S}, ℓ_2) is a compact metric space, and \mathcal{P} is closed, bounded, and equicontinuous given by Assumption 2, we can see that \mathcal{P} is compact by Lemma 1.

We next need to prove that the loss function $\mathcal{J}(p(\delta_i), \theta)$ is continuously differentiable with respect to both $p(\delta_i)$ and θ , i.e., the gradient $\nabla_{\theta} \mathcal{J}(p(\delta_i), \theta)$ is joint continuous on $\mathcal{P} \times \mathbb{R}^m$, where m is the dimension of θ .

To prove it, we first define a new metric on $\mathcal{P} \times \mathbb{R}^m$ as

$$d_{mix}((p_1, \theta_1), (p_2, \theta_2)) = d_C(p_1, p_2) + \ell_2(\theta_1, \theta_2).$$

Then $(\mathcal{P} \times \mathbb{R}^m, d_{mix})$ is a new metric space.

By definition, given a point $(p_0, \theta_0) \in \mathcal{P} \times \mathbb{R}^m$, if for each $\tau > 0$, there is a $\gamma > 0$, such that

$$\ell_2(\nabla_{\theta} \mathcal{J}(p(\delta_i), \theta), \nabla_{\theta} \mathcal{J}(p_0(\delta_i), \theta_0)) < \tau$$

whenever $d_{mix}((p, \theta), (p_0, \theta_0)) < \gamma$, then the function $\nabla_{\theta} \mathcal{J}(p(\delta_i), \theta)$ is continuous at (p_0, θ_0) . If for all points in $\mathcal{P} \times \mathbb{R}^m$, the function is continuous, then $\nabla_{\theta} \mathcal{J}(p(\delta_i), \theta)$ is continuous on $\mathcal{P} \times \mathbb{R}^m$.

To show that, we first have

$$\begin{aligned} & \ell_2(\nabla_{\theta} \mathcal{J}(p(\delta_i), \theta), \nabla_{\theta} \mathcal{J}(p_0(\delta_i), \theta_0)) \\ & \leq \ell_2(\nabla_{\theta} \mathcal{J}(p(\delta_i), \theta), \nabla_{\theta} \mathcal{J}(p(\delta_i), \theta_0)) \\ & \quad + \ell_2(\nabla_{\theta} \mathcal{J}(p(\delta_i), \theta_0), \nabla_{\theta} \mathcal{J}(p_0(\delta_i), \theta_0)). \end{aligned} \quad (\text{A.1})$$

We already have that the loss function $\mathcal{J}(p(\delta_i), \theta)$ is continuously differentiable with respect to θ by Assumption 1. Then given $\frac{\tau}{2}$, there is a γ_1 , such that

$$\ell_2(\nabla_{\theta} \mathcal{J}(p(\delta_i), \theta), \nabla_{\theta} \mathcal{J}(p(\delta_i), \theta_0)) < \frac{\tau}{2}$$

whenever $\ell_2(\theta, \theta_0) < \gamma_1$.

For the second term of the RHS of Eqn. (A.1), we have

$$\begin{aligned} & \ell_2(\nabla_{\theta} \mathcal{J}(p(\delta_i), \theta_0), \nabla_{\theta} \mathcal{J}(p_0(\delta_i), \theta_0)) \\ & = \|\nabla_{\theta} (\mathcal{J}(p(\delta_i), \theta_0) - \mathcal{J}(p_0(\delta_i), \theta_0))\|_2 \\ & = \left\| \int_{\mathcal{S}} (p(\delta_i) - p_0(\delta_i)) \nabla_{\theta} \mathcal{L}(f_{\theta}(\mathbf{x}_i + \delta_i), y_i) d\delta_i \right\|_2 \\ & \leq d_C(p, p_0) \cdot \int_{\mathcal{S}} \|\nabla_{\theta} \mathcal{L}(f_{\theta}(\mathbf{x}_i + \delta_i), y_i)\|_2 d\delta_i. \end{aligned}$$

Therefore, for the given $\frac{\tau}{2}$, there is also a γ_2 which equals to

$$\gamma_2 = \frac{\tau}{2 \int_{\mathcal{S}} \|\nabla_{\theta} \mathcal{L}(f_{\theta}(\mathbf{x}_i + \delta_i), y_i)\|_2 d\delta_i},$$

such that

$$\ell_2(\nabla_{\theta} \mathcal{J}(p(\delta_i), \theta_0), \nabla_{\theta} \mathcal{J}(p_0(\delta_i), \theta_0)) < \frac{\tau}{2}$$

whenever $d_C(p, p_0) < \gamma_2$.

Combining the results, for a given $\tau > 0$, we can set $\gamma = \gamma_1 + \gamma_2$, such that

$$\ell_2(\nabla_{\theta} \mathcal{J}(p(\delta_i), \theta), \nabla_{\theta} \mathcal{J}(p_0(\delta_i), \theta_0)) < \tau$$

whenever $d_{mix}((p, \theta), (p_0, \theta_0)) < \gamma$. Thus we have proven that the loss function $\mathcal{J}(p(\delta_i), \theta)$ is continuously differentiable with respect to both $p(\delta_i)$ and θ .

Given the above results, we can directly apply Danskin's theorem (Danskin, 2012) to prove Theorem 1. We state the Danskin's theorem in the following lemma.

Lemma 2. (Danskin's Theorem) Let \mathcal{Q} be a nonempty compact topological space and $h : \mathcal{Q} \times \mathbb{R}^m \rightarrow \mathbb{R}$ be a function satisfying that $h(q, \cdot)$ is differentiable for every $q \in \mathcal{Q}$ and $\nabla_{\theta} h(q, \theta)$ is continuous on $\mathcal{Q} \times \mathbb{R}^m$. We define $\Psi(\theta) = \max_{q \in \mathcal{Q}} h(q, \theta)$, and $\mathcal{Q}^*(\theta) = \{q \in \mathcal{Q} : h(q, \theta) = \Psi(\theta)\}$. Then $\Psi(\theta)$ is directionally differentiable, and its directional derivative along the direction \mathbf{v} satisfies

$$\Psi'(\theta; \mathbf{v}) = \sup_{q \in \mathcal{Q}^*(\theta)} \mathbf{v}^{\top} \nabla_{\theta} h(q, \theta).$$

In particular, when the set $\mathcal{Q}^*(\theta) = \{q^*\}$ only contains one maximizer, $\Psi(\theta)$ is differentiable at θ and

$$\nabla_{\theta} \Psi(\theta) = \nabla_{\theta} h(q^*, \theta).$$

If we let $\mathcal{Q} = \mathcal{P}$ and $h = \mathcal{J}$ in Lemma 2, we can directly prove Theorem 1. \square

A.2. Proof of Eqn. (11)

The variable δ_i has the following sampling process

$$\delta_i = \epsilon \cdot \tanh(\mathbf{u}_i), \quad \mathbf{u}_i \sim \mathcal{N}(\boldsymbol{\mu}_i, \text{diag}(\boldsymbol{\sigma}_i^2)),$$

whose negative log density is

$$\begin{aligned} & \sum_{j=1}^d \left(\frac{1}{2} (\mathbf{r}^{(j)})^2 + \frac{\log 2\pi}{2} + \log \sigma_i^{(j)} \right) \\ & + \log(1 - \tanh(\boldsymbol{\mu}_i^{(j)} + \boldsymbol{\sigma}_i^{(j)} \mathbf{r}^{(j)})^2) + \log \epsilon, \end{aligned}$$

where the superscript j denotes the j -th element of a vector.

Proof. Due to the usage of the diagonal covariance matrix, each dimension in the sampled perturbation δ_i is independent. Thus we can simply calculate the negative log density in each dimension of δ_i . For clarity, we also denote

$\mu_i^{(j)}$, $\sigma_i^{(j)}$, $\mathbf{r}^{(j)}$, $\mathbf{u}_i^{(j)}$, and $\delta_i^{(j)}$ as μ , σ , r , u , and δ , respectively. Based on the sampling procedure in Eqn. (9), we have $\delta = \epsilon \cdot \tanh(u)$ and $u = \mu + \sigma r$.

Note that r has density: $p(r) = \frac{1}{\sqrt{2\pi}} \exp(-\frac{r^2}{2})$. Apply the *transformation of variable* approach, we have the density of u as

$$\begin{aligned} p(u) &= \frac{1}{\sqrt{2\pi}} \exp(-\frac{r^2}{2}) \cdot \left| \frac{d}{du} \left(\frac{u - \mu}{\sigma} \right) \right| \\ &= \frac{1}{\sqrt{2\pi}\sigma} \exp(-\frac{r^2}{2}). \end{aligned}$$

Let $\beta = \tanh(u)$, then the inverse transformation is $u = \tanh^{-1}(\beta) = \frac{1}{2} \log(\frac{1+\beta}{1-\beta})$, whose derivative with respect to β is $\frac{1}{1-\beta^2}$.

Then, by applying the *transformation of variable* approach again, we have the density of β as

$$\begin{aligned} p(\beta) &= \frac{1}{\sqrt{2\pi}\sigma} \exp(-\frac{r^2}{2}) \cdot \frac{1}{1-\beta^2} \\ &= \frac{1}{\sqrt{2\pi}\sigma} \exp(-\frac{r^2}{2}) \cdot \frac{1}{1 - \tanh(\mu + \sigma r)^2}. \end{aligned}$$

Therefore, the density of δ which equals to $\epsilon \cdot \beta$ can be derived similarly, and eventually we obtain

$$p(\delta) = \frac{1}{\sqrt{2\pi}\sigma} \exp(-\frac{r^2}{2}) \cdot \frac{1}{1 - \tanh(\mu + \sigma r)^2} \cdot \frac{1}{\epsilon}.$$

Consequently, the negative log density of $p(\delta)$ is

$$\begin{aligned} -\log p(\delta) &= \frac{r^2}{2} + \frac{\log 2\pi}{2} + \log \sigma \\ &\quad + \log(1 - \tanh(\mu + \sigma r)^2) + \log \epsilon. \end{aligned}$$

Sum over all of the dimensions and we complete the proof of Eqn. (11). \square

A.3. Proof of Eqn. (14)

Given an example \mathbf{x}_i , we define an implicit distribution in the form of $\delta_i = g_\phi(\mathbf{z}; \mathbf{x}_i)$, $\mathbf{z} \sim p(\mathbf{z})$, where g_ϕ denotes a ϕ -parameterized generator network. Then we can maximize the following variational lower bound to maximize the entropy of this distribution

$$\mathcal{H}(p_\phi(\delta_i|\mathbf{x}_i)) \geq \mathcal{U}(q) = \mathbb{E}_{p(\mathbf{z})} \log q(\mathbf{z}|g_\phi(\mathbf{z}; \mathbf{x}_i)) + c$$

where c is a constant and $q(\cdot|\cdot)$ is a variational distribution.

Proof. We mainly follow Dai et al. (2017a) to provide the proof. Typically, we can view the Dirac generation distribution $p_\phi(\delta_i|\mathbf{x}_i, \mathbf{z})$ as a peaked Gaussian with a fixed, diagonal covariance, then it will have a constant entropy. Considering \mathbf{x}_i as a given condition, we can simply rewrite

the generation distribution as $p_{\phi,i}(\delta_i|\mathbf{z})$. Then we can define the joint distribution over δ_i and \mathbf{z} as $p_{\phi,i}(\delta_i, \mathbf{z}) = p_{\phi,i}(\delta_i|\mathbf{z})p_{\phi,i}(\mathbf{z})$. $p_{\phi,i}(\mathbf{z}) = p(\mathbf{z})$ is simply a predefined prior with a constant entropy. Then, we can further define the marginal $p_{\phi,i}(\delta_i)$ whose entropy is of our interest and the posterior $p_{\phi,i}(\mathbf{z}|\delta_i)$. Consider the mutual information between δ_i and \mathbf{z}

$$\begin{aligned} \mathcal{I}(p_{\phi,i}(\delta_i); p_{\phi,i}(\mathbf{z})) &= \mathcal{H}(p_{\phi,i}(\delta_i)) - \mathcal{H}(p_{\phi,i}(\delta_i|\mathbf{z})) \\ &= \mathcal{H}(p_{\phi,i}(\mathbf{z})) - \mathcal{H}(p_{\phi,i}(\mathbf{z}|\delta_i)). \end{aligned}$$

Thus, we can calculate the entropy of δ_i as

$$\mathcal{H}(p_{\phi,i}(\delta_i)) = \mathcal{H}(p_{\phi,i}(\mathbf{z})) - \mathcal{H}(p_{\phi,i}(\mathbf{z}|\delta_i)) + \mathcal{H}(p_{\phi,i}(\delta_i|\mathbf{z})).$$

As stated, the first term and the last term are constant with respect to the parameter ϕ . Therefore, maximizing $\mathcal{H}(p_{\phi,i}(\delta_i))$ corresponds to maximizing the negative conditional entropy

$$-\mathcal{H}(p_{\phi,i}(\mathbf{z}|\delta_i)) = \mathbb{E}_{\delta_i \sim p_{\phi,i}(\delta_i)} [\mathbb{E}_{\mathbf{z} \sim p_{\phi,i}(\mathbf{z}|\delta_i)} [\log p_{\phi,i}(\mathbf{z}|\delta_i)]].$$

We still cannot optimize this as we have no access to the posterior. As an alternative, we resort to the variational inference technique to tackle this problem. We introduce a variational distribution $q(\mathbf{z}|\delta_i)$ to approximate the true posterior, and derive the following lower bound

$$\begin{aligned} -\mathcal{H}(p_{\phi,i}(\mathbf{z}|\delta_i)) &= \mathbb{E}_{\delta_i \sim p_{\phi,i}(\delta_i)} [\mathbb{E}_{\mathbf{z} \sim p_{\phi,i}(\mathbf{z}|\delta_i)} [\log q(\mathbf{z}|\delta_i)]] \\ &\quad + \mathcal{D}_{KL}(p_{\phi,i}(\mathbf{z}|\delta_i) || q(\mathbf{z}|\delta_i)) \\ &\geq \mathbb{E}_{\delta_i \sim p_{\phi,i}(\delta_i)} [\mathbb{E}_{\mathbf{z} \sim p_{\phi,i}(\mathbf{z}|\delta_i)} [\log q(\mathbf{z}|\delta_i)]] \\ &= \mathbb{E}_{\mathbf{z}, \delta_i \sim p_{\phi,i}(\mathbf{z}, \delta_i)} [\log q(\mathbf{z}|\delta_i)] \\ &= \underbrace{\mathbb{E}_{\mathbf{z} \sim p_{\phi,i}(\mathbf{z})} [\mathbb{E}_{\delta_i \sim p_{\phi,i}(\delta_i|\mathbf{z})} [\log q(\mathbf{z}|\delta_i)]]}_{\mathcal{U}'(q)}, \end{aligned}$$

where \mathcal{D}_{KL} represents the KullbackLeibler divergence between distributions. Note that $p_{\phi,i}(\mathbf{z}) = p(\mathbf{z})$ is a prior and $p_{\phi,i}(\delta_i|\mathbf{z}) = p_\phi(\delta_i|\mathbf{x}_i, \mathbf{z})$ is Dirac distribution located at $\delta_i = g_\phi(\mathbf{z}; \mathbf{x}_i)$. Thus, we can write the lower bound of the entropy $\mathcal{U}(q)$ as

$$\begin{aligned} \mathcal{H}(p_\phi(\delta_i|\mathbf{x}_i)) &\geq \mathcal{U}(q) = \mathcal{U}'(q) + c \\ &= \mathbb{E}_{\mathbf{z} \sim p(\mathbf{z})} \log q(\mathbf{z}|g_\phi(\mathbf{z}; \mathbf{x}_i)) + c, \end{aligned}$$

which can be optimized effectively via Monte Carlo integration and standard back-propagation. Then we finish the proof of Eqn. (14). \square

B. Algorithms

In this section, we present the three proposed algorithms in detail.

B.1. Algorithm for ADT_{EXP}

We provide the algorithm for training ADT_{EXP} in Alg. 2.

Algorithm 2 The training algorithm for ADT_{EXP}

```

1: Input: Training data  $\mathcal{D}$ , objective  $\mathcal{J}(p_{\phi_i}(\delta_i), \theta)$ , training epochs  $N$ , the number of inner maximization steps  $T$ , the number of MC samples for gradient estimation in each step  $k$ , and learning rates  $\eta_\theta, \eta_\phi$ .
2: Initialize  $\theta$ ;
3: for epoch = 1 to  $N$  do
4:   for each minibatch  $\mathcal{B} \subset \mathcal{D}$  do
5:     for each input  $(\mathbf{x}_i, y_i) \in \mathcal{B}$  do
6:       Initialize  $\phi_i$ ;
7:       for  $t = 1$  to  $T$  do
8:         Calculate the gradient  $\mathbf{g}_i$  of  $\phi_i$  by Eqn. (10) via MC integration using  $k$  samples;
9:         Update  $\phi_i$  with gradient ascent
            
$$\phi_i \leftarrow \phi_i + \eta_\phi \cdot \mathbf{g}_i.$$

10:      end for
11:    end for
12:    Update  $\theta$  with stochastic gradient descent
            
$$\theta \leftarrow \theta - \eta_\theta \cdot \mathbb{E}_{(\mathbf{x}_i, y_i) \in \mathcal{B}} [\nabla_\theta \mathcal{J}(p_{\phi_i}(\delta_i), \theta)].$$

13:  end for
14: end for
    
```

B.2. Algorithm for $\text{ADT}_{\text{EXP-AM}}$

We provide the algorithm for training $\text{ADT}_{\text{EXP-AM}}$ in Alg. 3.

B.3. Algorithm for $\text{ADT}_{\text{IMP-AM}}$

We provide the algorithm for training $\text{ADT}_{\text{IMP-AM}}$ in Alg. 4.

C. Detailed Experimental Settings

We provide the detailed experimental settings in this section.

C.1. Datasets

We choose the CIFAR-10, CIFAR-100 (Krizhevsky & Hinton, 2009), and SVHN (Netzer et al., 2011) datasets to conduct the experiments. CIFAR consists of a training set of 50,000 and a test set of 10,000 color images of resolution 32×32 with 10 classes in CIFAR-10 and 100 classes in CIFAR-100. SVHN is a 10-class house number classification dataset with 73,257 training images and 26,032 test images. During training, we perform standard data augmentation (i.e., horizontal flips and random crops from images with 4 pixels padded on each side) on CIFAR-10 and CIFAR-100, and use no data augmentation on SVHN. We do not use any data augmentation during testing.

C.2. Network Architectures

For the generator network in $\text{ADT}_{\text{EXP-AM}}$ and $\text{ADT}_{\text{IMP-AM}}$, we adopt a popular image-to-image architecture which has

Algorithm 3 The training algorithm for $\text{ADT}_{\text{EXP-AM}}$

```

1: Input: Training data  $\mathcal{D}$ , objective function in Eqn. (12), training epochs  $N$ , and learning rates  $\eta_\theta, \eta_\phi$ .
2: Initialize  $\theta$  and  $\phi$ ;
3: for epoch = 1 to  $N$  do
4:   for each minibatch  $\mathcal{B} \subset \mathcal{D}$  do
5:     Input  $\mathbf{x}_i$  to the generator and obtain the distribution parameters  $(\mu_i, \sigma_i)$  for each  $(\mathbf{x}_i, y_i) \in \mathcal{B}$ ;
6:     Sample one  $\delta_i$  from the distribution defined by Eqn. (9) given  $(\mu_i, \sigma_i)$  for each  $(\mathbf{x}_i, y_i) \in \mathcal{B}$  to approximately calculate the gradient of Eqn. (12) with respect to  $\theta$  and  $\phi$ , and obtain  $\mathbf{g}_\theta$  and  $\mathbf{g}_\phi$ ;
7:     Update  $\theta$  by:  $\theta \leftarrow \theta - \eta_\theta \cdot \mathbf{g}_\theta$ .
8:     Update  $\phi$  by:  $\phi \leftarrow \phi + \eta_\phi \cdot \mathbf{g}_\phi$ .
9:   end for
10: end for
    
```

Algorithm 4 The training algorithm for $\text{ADT}_{\text{IMP-AM}}$

```

1: Input: Training data  $\mathcal{D}$ , objective function in Eqn. (15), training epochs  $N$ , and learning rates  $\eta_\theta, \eta_\phi, \eta_\psi$ .
2: Initialize  $\theta, \phi$ , and  $\psi$ ;
3: for epoch = 1 to  $N$  do
4:   for each minibatch  $\mathcal{B} \subset \mathcal{D}$  do
5:     For each  $(\mathbf{x}_i, y_i) \in \mathcal{B}$ , sample a noise  $\mathbf{z}_i$  from  $\mathcal{U}(-1, 1)$ .
6:     Use the sampled noises to approximately calculate the gradient of Eqn. (15) with respect to  $\theta, \phi$ , and  $\psi$ , and obtain  $\mathbf{g}_\theta, \mathbf{g}_\phi$ , and  $\mathbf{g}_\psi$ .
7:     Update  $\theta$  by:  $\theta \leftarrow \theta - \eta_\theta \cdot \mathbf{g}_\theta$ .
8:     Update  $\phi$  by:  $\phi \leftarrow \phi + \eta_\phi \cdot \mathbf{g}_\phi$ .
9:     Update  $\psi$  by:  $\psi \leftarrow \psi + \eta_\psi \cdot \mathbf{g}_\psi$ .
10:   end for
11: end for
    
```

shown promise in neural style transfer and super-resolution (Johnson et al., 2016; Zhu et al., 2017). The network contains 3 residual blocks (He et al., 2016), with two extra convolutions at the beginning and the end. All convolutions in the generator have stride 1, and are immediately followed by batch normalization (Ioffe & Szegedy, 2015) and ReLU activation.

As found by Chen et al. (2018), taking only the natural images as inputs to the generator network can lead to poor results. And they suggest to input the classifier’s gradients as well. Based on this finding, we calculate the gradient of the loss function at the natural input $\mathbf{g}_i^1 = \nabla_{\mathbf{x}} \mathcal{L}(f_\theta(\mathbf{x}_i), y_i)$, as well as the gradient of the loss function at the FGSM adversarial example $\mathbf{g}_i^2 = \nabla_{\mathbf{x}} \mathcal{L}(f_\theta(\mathbf{x}_i + \delta_i^{\text{FGSM}}), y_i)$, where $\delta_i^{\text{FGSM}} = \epsilon \cdot \text{sign}(\nabla_{\mathbf{x}} \mathcal{L}(f_\theta(\mathbf{x}_i), y_i))$, and then input $[\mathbf{x}_i, \mathbf{g}_i^1, \mathbf{g}_i^2]$ to the generator network.

In $\text{ADT}_{\text{EXP-AM}}$, the generator has 6 output channels to deliver the parameters (i.e., mean and standard derivation) of

Table 5. The network architectures used for the generators.

In ADT _{EXP-AM}	In ADT _{IMP-AM}
input	z
256 × 3 × 3 conv	256-dim fc layer
Residual block, 512 filters	1024-dim fc layer
Residual block, 512 filters	reshape to 1 × 32 × 32
Residual block, 512 filters	concat with input
6 × 3 × 3 conv	256 × 3 × 3 conv
	Residual block, 512 filters
	Residual block, 512 filters
	Residual block, 512 filters
	3 × 3 × 3 conv

 Table 6. The network architecture used for instantiating the variational distribution q in ADT_{IMP-AM}.

Layers
input
32 × 5 × 5, stride 1
64 × 4 × 4, stride 2
128 × 4 × 4, stride 1
256 × 4 × 4, stride 2
Global average pooling
128 × 1 × 1, stride 1

the explicit adversarial distributions. In ADT_{IMP-AM}, for each input we sample a 64-dim i.i.d. \mathbf{z} from a uniform distribution $U(-1, 1)$, which is encoded with 2 fully connected (FC) layers and then fed into the generator along with the input image and gradients.

We elaborate the architectures of the generator networks in Table 5, and the architecture of q in ADT_{IMP-AM} in Table 6. In these tables, “C×H×W” means a convolutional layer with C filters size H×W, which is followed by batch normalization (Ioffe & Szegedy, 2015) and a ReLU nonlinearity (or LeakyReLU for layers in Table 6), except the last layers in the architectures. We use the residual block design of He et al. (2016), which is composed of two 3 × 3 convolutions and a residual connection.

C.3. Training Details

The classifier is trained using SGD with momentum 0.9, weight decay 2×10^{-4} , and batch size 64. The initial learning rate is 0.1, which is reduced to 0.01 in the 75-th epoch. We stop training after 76 epochs. For ADT_{EXP}, we adopt Adam (Kingma & Ba, 2015) for optimizing the distribution parameters ϕ_i . We set the learning rate for ϕ_i as 0.3, the momentum as (0.0, 0.0), the number of optimization steps as $T = 7$, and the number of MC samples to estimate the gradient in each step as $k = 5$. For ADT_{EXP-AM} and ADT_{IMP-AM}, we use only one MC sample for gradient estimation and use Adam with momentum (0.5, 0.999) and learning rate 2×10^{-4} to optimize the parameter ϕ of the generator network. We also adopt Adam with learning rate 2×10^{-4} to optimize the parameter ψ of the introduced

variational in ADT_{IMP-AM}.

C.4. Baselines

Our primary baselines include: 1) standard training on the clean images (**Standard**); 2) adversarial training on the PGD adversarial examples (AT_{PGD}) (Madry et al., 2018). Standard and AT_{PGD} are trained with the same configurations specified above. For training AT_{PGD}, we perform PGD with $T = 7$ steps, and step size $\alpha = \epsilon/4$, which are the same as in Madry et al. (2018). On CIFAR-10, we incorporate several additional baselines, including: 1) adversarial training on the targeted FGSM adversarial examples (AT_{FGSM}) (Kurakin et al., 2017); 2) adversarial logit pairing (ALP) (Kannan et al., 2018); and 3) feature scattering-based adversarial training (**FeaScatter**) (Zhang & Wang, 2019). We implement AT_{FGSM} and ALP by ourselves using the same training configuration specified above and use the pretrained model of FeaScatter. Note that all of these models have the same network architecture for a fair comparison.

C.5. A Feature Attack for White-box Evaluation

We incorporate a feature attack (FeaAttack)⁴ for white-box robustness evaluation in this paper. The algorithm of FeaAttack is introduced below. Given a natural input \mathbf{x} , FeaAttack first finds a target image \mathbf{x}' belonging to a different class. It minimizes the cosine similarity between the feature representations of the adversarial example and \mathbf{x}' as

$$\delta^* = \arg \min_{\delta \in \mathcal{S}} \mathcal{L}_{\cos}(f'_{\theta}(\mathbf{x} + \delta), f'_{\theta}(\mathbf{x}')),$$

where $f'_{\theta}(\cdot)$ returns the feature representation before the global average pooling layer for an input, and \mathcal{L}_{\cos} is the cosine similarity between two features. FeaAttack solves this objective function by

$$\delta^{t+1} = \Pi_{\mathcal{S}}(\delta^t - \alpha \cdot \text{sign}(\nabla_{\mathbf{x}} \mathcal{L}_{\cos}(f'_{\theta}(\mathbf{x} + \delta^t), f'_{\theta}(\mathbf{x}')))).$$

δ^0 is initialized uniformly in \mathcal{S} . In our experiments, we set $\alpha = \epsilon/8$ and the number of optimization steps as 50. For each natural input, we randomly select 200 target images to conduct 200 attacks, and report a successful attack when one of them can cause misclassification of the model.

D. Supplementary Experimental Results

We provide more experimental results in this section.

D.1. Convergence of Learning the Explicit Adversarial Distributions

We study the convergence of the explicit adversarial distributions introduced in Section 3.1 by attacking AT_{PGD} and

⁴<https://github.com/Line290/FeatureAttack>.

Table 7. Classification accuracy of TRADES (Zhang et al., 2019) and the three ADT-based methods trained with the TRADES loss on CIFAR-10 under white-box attacks with $\epsilon = 8/255$. We mark the best results for each attack and the overall results that outperform TRADES in **bold**, and the overall best result in **blue**.

Model	\mathcal{A}_{nat}	FGSM	PGD-20	PGD-100	MIM	C&W	FeaAttack	\mathcal{A}_{rob}
TRADES	83.89%	59.79%	53.92%	53.68%	54.78%	52.71%	54.38%	51.67%
ADT _{EXP} w. TRADES	84.89%	60.23%	54.96%	54.56%	55.72%	52.96%	54.96%	52.13%
ADT _{EXP-AM} w. TRADES	84.86%	60.43%	55.22%	55.00%	55.68%	52.30%	57.91%	51.77%
ADT _{IMP-AM} w. TRADES	83.95%	65.61%	55.87%	54.79%	54.14%	52.82%	58.80%	51.81%

ADT_{EXP} with different attack iterations. We set the learning rate of ϕ_i as 0.3, the momentum as (0.0, 0.0), the number of MC samples to estimate the gradient in each step as $k = 10$, and vary the attack iterations from 0 to 100. We show the classification loss and accuracy in Figure 5. Learning the explicit adversarial distributions can converge soon within a few iterations.

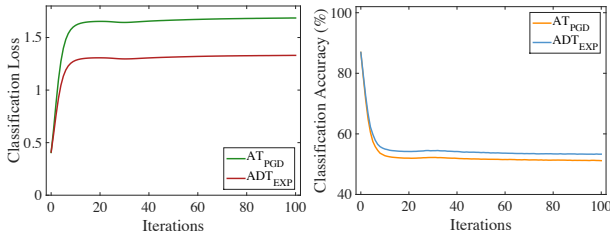


Figure 5. Classification loss (i.e., cross-entropy loss) and accuracy (%) of AT_{PGD} and ADT_{EXP} under the explicit adversarial distributions attack with different attack iterations.

D.2. Training Time

We provide the training time for one epoch of Standard, AT_{PGD}, ADT_{EXP}, ADT_{EXP-AM}, and ADT_{IMP-AM} on CIFAR-10 in Figure 6. As can be seen, ADT_{EXP} is nearly $5\times$ slower than AT_{PGD} since we use $k = 5$ MC samples to estimate the gradient with respect to the distribution parameters in each step. Nevertheless, by amortizing the adversarial distributions, ADT_{EXP-AM} and ADT_{IMP-AM} are much faster than ADT_{EXP}, and nearly $2\times$ faster than AT_{PGD}.

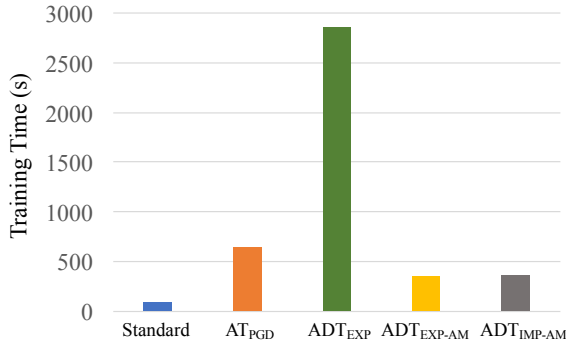


Figure 6. The training time (s) for one epoch of Standard, AT_{PGD}, ADT_{EXP}, ADT_{EXP-AM}, and ADT_{IMP-AM} on CIFAR-10.

D.3. Comparison with Zhang et al. (2019)

Although we use the cross-entropy loss as our training objective in most of the experiments, our proposed ADT framework is compatible with other loss functions. As a concrete example, we integrate TRADES (Zhang et al., 2019) with ADT. In TRADES, the minimax optimization problem is formulated as

$$\min_{\theta} \frac{1}{n} \sum_{i=1}^n \left\{ \mathcal{L}(f_{\theta}(\mathbf{x}_i), y_i) + \max_{\delta_i \in \mathcal{S}} \mathcal{L}(f_{\theta}(\mathbf{x}_i + \delta_i), f_{\theta}(\mathbf{x}_i)) / \lambda' \right\},$$

where \mathcal{L} is the cross-entropy loss⁵, λ' is a different hyperparameter from λ in our proposed method. We similarly implement ADT with TRADES by replacing the loss function in Eqn. (6) with the TRADES loss.

Since we use a smaller network architecture with 28 layers while Zhang et al. (2019) use a 34-layer Wide ResNet, we reimplement TRADES with WRN-28-10. We set $1/\lambda' = 6$ for all models. Table 7 shows the classification accuracy of TRADES and the three ADT-based methods trained with the TRADES loss on CIFAR-10 under white-box attacks. Our methods can also improve the robustness upon TRADES.

D.4. Comparison with Chen et al. (2018)

We further compare ADT with the L2L framework in Chen et al. (2018). Their method is similar to ours in the sense that they also adopt a generator network to produce adversarial examples, and perform adversarial training on those generated adversarial examples. The essential different between our methods and theirs is that we propose an adversarial distributional training framework to learn the distributions of adversarial perturbations, while their method is a variant of the vanilla adversarial training with a different approach to solving the inner maximization.

Since the source code is not provided by Chen et al. (2018), we tried to reproduce their reported results with the same training configuration specified in their paper, but we failed. Therefore, we adopt the same configuration as in ADT for training the L2L model. Table 8 shows the results of L2L, ADT_{EXP-AM}, and ADT_{IMP-AM}, which use the same classifier

⁵In the code provided by Zhang et al. (2019), the second term is implemented by the KL divergence.

Table 8. Classification Accuracy of L2L (Chen et al., 2018), $\text{ADT}_{\text{EXP-AM}}$, and $\text{ADT}_{\text{IMP-AM}}$ on CIFAR-10 under white-box attacks with $\epsilon = 8/255$.

Model	L2L	$\text{ADT}_{\text{EXP-AM}}$	$\text{ADT}_{\text{IMP-AM}}$
\mathcal{A}_{nat}	88.15%	87.82%	88.00%
FGSM	65.50%	62.42%	64.89%
PGD-20	48.55%	51.95%	52.28%
PGD-100	47.14%	51.26%	51.23%
MIM	49.03%	52.99%	52.64%
C&W	49.22%	51.75%	52.65%

architecture and generator network. Our ADT-based methods outperform L2L in most cases, showing the advantages of learning the distributions of adversarial perturbations upon finding a single adversarial example.